

Enhanced spin-orbit optical mirages from dual nanospheres

Jorge Olmos-Trigo,¹ Cristina Sanz-Fernández,² Aitzol García-Etxarri,^{1,2} Gabriel Molina-Terriza,^{1,2,3} F. Sebastián Bergeret,^{1,2} and Juan José Sáenz^{1,3,*}

¹*Donostia International Physics Center (DIPC), 20018 Donostia-San Sebastián, Spain*

²*Centro de Física de Materiales (CFM-MPC), Centro Mixto CSIC-UPV/EHU, 20018 Donostia-San Sebastián, Spain*

³*IKERBASQUE, Basque Foundation for Science, 48013 Bilbao, Spain*

Spin-orbit interaction of light can lead to the so-called optical mirages, i.e. a perceived displacement in the position of a particle due to the spiraling structure of the scattered light. In electric dipoles, the maximum displacement is subwavelength and does not depend on the optical properties of the scatterer. Here we will show that the optical mirage in high refractive index dielectric nanoparticles depends strongly on the ratio between electric and magnetic dipolar responses. When the dual symmetry is satisfied (at the first Kerker condition), there is a considerable enhancement (far above the wavelength) of the spin-orbit optical mirage which can be related to the emergence of an optical vortex in the backscattering direction.

It is customary to separate the angular momentum (AM) of light [1] into two contributions, the spin (SAM) and the orbital angular momentum (OAM), that can be coupled by light propagation and scattering. The study of this spin-orbit interaction (SOI) has attracted a great deal of interest in the past years [2–5].

An interesting analogy between the SOI in light and the spin Hall effect (SHE) in electronic systems can be drawn [6, 7]. In the latter, electrons with different spins are deflected differently by scattering off impurities due to the SOI. This leads to a transversal spin current that in turn induces a measurable spin accumulation at the sample edges. One of the microscopic origins of the SHE is the so-called side-jump mechanism [8], in which a spin-dependent displacement of the center of mass of the electronic wave packet takes place due to the SOI (for more details we refer to the reviews [9, 10]).

Similarly, an apparent transversal displacement of a target particle induced by light scattering can be explained by an AM exchange. Hereafter this effect is referred to as *optical mirage* and has been observed in several situations, for example, in beams impinging on a dielectric surface [11–13] or when considering a spherical target described by a single electric polarizability [14]. In the latter case, the apparent shift of the dipole localization does not depend on the optical properties, but on the scattering angle, with opposite displacements for incident left and right circularly polarized photons (spins). The apparent shift (Δ) is maximized at the plane perpendicular to the direction of the incoming wave taking a value of $\Delta = \lambda/\pi$ and thus, it is always subwavelength.

In this Letter, we demonstrate that by taking into account both, the electric and magnetic dipoles sustained by a high refractive index spherical particle, the subwavelength maximum limit can be drastically surpassed when the particle is excited by circularly polarized light. In other words, a large macroscopic apparent shift ($\Delta \gg \lambda$) is induced in the back scattering region. Specifically, we

show that this optical mirage is related to the generation of a spiraling power flow and can be explained in terms of an angular momentum redistribution per photon between the SAM and OAM contributions. Based on helicity conservation we predict an intriguing enhancement of the momentum transfer when the system is dual, i.e. when the electric and magnetic dipolar moments are equal. At this, so-called, “first Kerker condition” [15–17], the emitted light intensity vanishes in the backscattering direction, leading to the appearance of a (2σ charge) topological optical vortex.

We consider a non-absorbing dielectric sphere of radius a and refractive index n_p embedded in an otherwise homogeneous medium with constant and real refractive index n_h . The geometry of the scattering problem is sketched in Fig. 1, where we consider a circularly polarized plane wave with wavenumber $k = n_h k_0 = n_h 2\pi/\lambda_0$ (being λ_0 the light wavelength in vacuum) and helicity $\sigma = \pm 1$ (we associate left polarized light with a positive helicity $\sigma = +1$) incident along the z -axis. Instead of using the traditional multipole Mie expansion to describe the light scattered by the sphere [18, 19], we shall find it useful to work in a basis of multipoles, eigenfunctions, Ψ_{lm}^σ , of the helicity operator Λ , [20, 21],

$$\Lambda \Psi_{lm}^\sigma = (1/k) \nabla \times \Psi_{lm}^\sigma = \sigma \Psi_{lm}^\sigma,$$

with

$$\Psi_{lm}^\sigma = \frac{1}{\sqrt{2}} \left[\frac{\nabla \times g_l(kr) \mathbf{X}_{lm}}{k} + \sigma g_l(kr) \mathbf{X}_{lm} \right], \quad (1)$$

$$g_l(kr) = A_l^{(1)} h_l^{(1)}(kr) + A_l^{(2)} h_l^{(2)}(kr), \quad (2)$$

$$\mathbf{X}_{lm} = \frac{1}{\sqrt{l(l+1)}} \mathbf{L} Y_l^m(\theta, \varphi), \quad (3)$$

where, following Jackson’s notation [18], \mathbf{X}_{lm} denote the vector spherical harmonic, with $\mathbf{X}_{00} = 0$, $g_l(kr)$ is a linear combination of the spherical Hankel functions, $Y_l^m(\theta, \varphi)$ are the spherical harmonics and \mathbf{L} is the orbital angular momentum operator, $\mathbf{L} = -i(\mathbf{r} \times \nabla)$. In

* juanjo.saenz@dipc.org

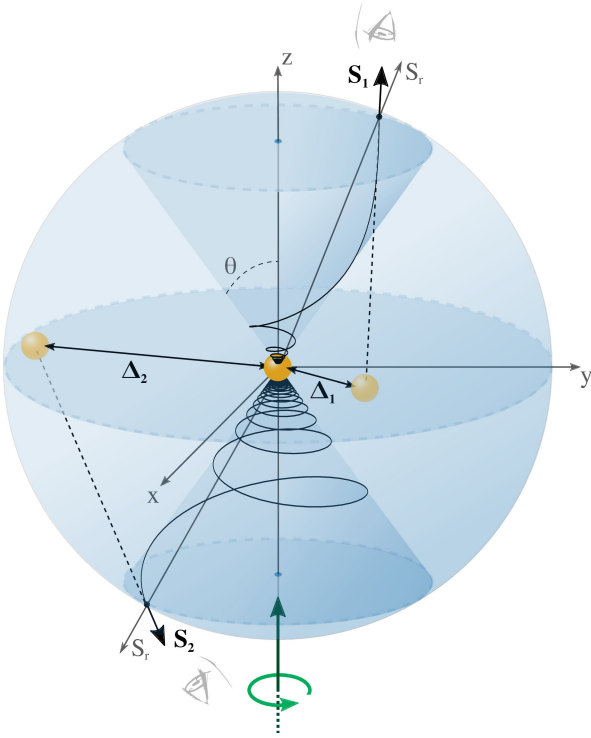


FIG. 1: Schematic representation of the optical mirage vector when considering a clockwise circularly polarized incoming wave (green straight arrow lying on the z -axis). The observer, represented by an eye, perceives a non-radial scattered Poynting vector ($\mathbf{S}_1, \mathbf{S}_2$) that leads to an apparent shift (Δ_1, Δ_2) of the dipole localization, both lying on the xy -plane.

this helicity basis, the incident field can be written as

$$\frac{\mathbf{E}_\sigma^{(0)}}{E_0} = \frac{\hat{x} + \sigma i \hat{y}}{\sqrt{2}} e^{ikz} = \sum_{l=0}^{\infty} \sum_{m=-l}^{+l} \sum_{\sigma'=\pm 1} C_{lm}^{\sigma\sigma'} \Psi_{lm}^{\sigma'}, \quad (4)$$

$$kZ\mathbf{H}_\sigma^{(0)} = -i\nabla \times \mathbf{E}_\sigma^{(0)}, \quad (5)$$

$$C_{lm}^{\sigma\sigma'} = \sigma i^l \sqrt{8\pi(2l+1)} \delta_{m\sigma} \delta_{\sigma\sigma'}, \quad (6)$$

where $1/Z = \epsilon_0 c n_h$ (being ϵ_0 and c the vacuum permittivity and speed of light, respectively) and $\Psi_{lm}^{\sigma'}$ is given by Eq. (1) with $g_l(kr) = j_l(kr)$. Such circularly polarized wave, with helicity σ , carries a $j_z = m = \sigma$ unit of total angular momentum per photon parallel to the propagation direction [18].

In the same basis, the scattered fields are given by

$$\frac{\mathbf{E}_\sigma^{\text{scat}}}{E_0} = \sum_{l=0}^{\infty} \sum_{m=-l}^{+l} \sum_{\sigma'=\pm 1} D_{lm}^{\sigma\sigma'} \Psi_{lm}^{\sigma'}, \quad (7)$$

$$D_{lm}^{\sigma\sigma'} = -i^l \sqrt{4\pi(2l+1)} \frac{\sigma a_l + \sigma' b_l}{2} \delta_{m\sigma}, \quad (8)$$

where now, since they are outgoing waves at infinity, $g_l(kr) = h_l^{(1)}(kr)$. Notice that a_l, b_l are the standard Mie electric and magnetic scattering coefficients [19]. Since a

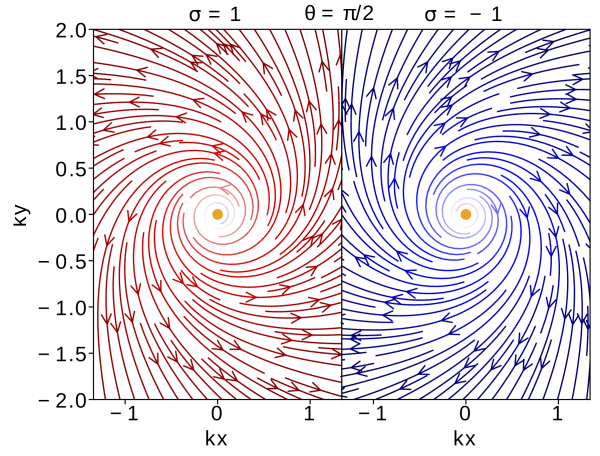


FIG. 2: Poynting vector streamlines with counterclockwise (clockwise) rotation for $\sigma = 1$ ($\sigma = -1$) when viewed from the perpendicular direction, $\theta = \pi/2$. This figure is valid for any dipolar response, i.e. arbitrary α_E and α_M . The orange circle represents the dipolar particle.

sphere presents axial symmetry around the z -axis, the j_z of the incident beam is preserved and the scattered wave can only involve $m = \sigma$. Consequently, $\mathbf{E}_\sigma^{\text{scat}}$ is an eigenfunction of the z -component of the total (dimensionless) angular momentum operator, $\mathbf{J} = \mathbf{L} + \mathbf{S}^{\text{spin}}$ (as well as of \mathbf{J}^2) [22], with eigenvalue $j_z = m = \sigma$,

$$\sigma = \frac{\mathbf{E}_\sigma^{\text{scat}*} \cdot (L_z + \mathbf{S}_z^{\text{spin}}) \mathbf{E}_\sigma^{\text{scat}}}{|\mathbf{E}_\sigma^{\text{scat}}|^2} = \ell_z(\mathbf{r}) + s_z(\mathbf{r}), \quad (9)$$

$$s_z(\mathbf{r}) = \frac{-i \{ \mathbf{E}_\sigma^{\text{scat}*} \times \mathbf{E}_\sigma^{\text{scat}} \} \cdot \hat{\mathbf{e}}_z}{|\mathbf{E}_\sigma^{\text{scat}}|^2} \quad (10)$$

$$\ell_z(\mathbf{r}) = \frac{\mathbf{E}_\sigma^{\text{scat}*} \cdot L_z \mathbf{E}_\sigma^{\text{scat}}}{|\mathbf{E}_\sigma^{\text{scat}}|^2} = \frac{-i}{|\mathbf{E}_\sigma^{\text{scat}}|^2} \left\{ \mathbf{E}_\sigma^{\text{scat}*} \cdot \frac{\partial \mathbf{E}_\sigma^{\text{scat}}}{\partial \varphi} \right\} \quad (11)$$

Equation (9) shows that the sum of the (dimensionless) OAM, $\ell_z(\mathbf{r})$, and SAM, $s_z(\mathbf{r})$, per photon is constant and equal to the helicity of the incoming plane wave. Notice that this is valid even in the near field region and it would be valid even in the presence of absorption. However, in general, the helicity is not preserved in the scattering process.

Let us now consider the scattering from a high refractive index (HRI) subwavelength sphere in a spectral range such that the optical response can be described by its first dipolar Mie coefficients a_1 and b_1 , i.e. by its electric and magnetic polarizabilities $\alpha_E = i a_1 (6\pi/k^3)$ and $\alpha_M = i b_1 (6\pi/k^3)$. The scattered field can be written as the sum of two components with opposite helicity,

$$\begin{aligned} \frac{\mathbf{E}_\sigma^{\text{scat}}}{E_0} &= -\frac{k^3}{\sqrt{6\pi}} \left\{ (\sigma \alpha_E + \alpha_M) \Psi_{1\sigma}^+ + (\sigma \alpha_E - \alpha_M) \Psi_{1\sigma}^- \right\} \\ &= \mathbf{E}_{\sigma+} + \mathbf{E}_{\sigma-}, \end{aligned} \quad (12)$$

which in far field limit become

$$\mathbf{E}_{\sigma\sigma'} \sim E_{\sigma\sigma'} e^{i\sigma\varphi} \left(\hat{\mathbf{e}}_{\sigma'} + i\sigma \frac{\sqrt{2}}{kr} \frac{\sigma \cos\theta - \sigma'}{\sin\theta} \hat{\mathbf{e}}_r + \dots \right) \quad (13)$$

where the last identity corresponds to the medium-far field expansion with

$$\frac{E_{\sigma\sigma'}}{E_0} = \frac{e^{ikr}}{4\pi kr} k^3 \left(\frac{\sigma\alpha_E + \sigma'\alpha_M}{2} \right) (\sigma \cos\theta + \sigma'), \quad (14)$$

$$\hat{\mathbf{e}}_{\sigma'} = \frac{1}{\sqrt{2}} (\hat{\mathbf{e}}_\theta + i\sigma' \hat{\mathbf{e}}_\varphi). \quad (15)$$

The scattered fields by HRI dielectric nanoparticles present a number of peculiar properties arising from the interference between the electric and magnetic dipolar radiation and have been largely discussed both theoretical and experimentally [23–29]. Most of these properties are encoded in the far-field radiation pattern, i.e. in the differential scattering cross section given by [16]

$$\begin{aligned} \frac{d\sigma_{\text{scat}}(\theta)}{d\Omega} &= \lim_{r \rightarrow \infty} r^2 \frac{\mathbf{S}^{\text{scat}} \cdot \hat{\mathbf{e}}_r}{|\mathbf{S}^{(0)}|} = r^2 \frac{|E_{\sigma+}|^2 + |E_{\sigma-}|^2}{|E_0|^2} \\ &= \frac{k^4 |\alpha_{\text{sum}}|^2}{(4\pi)^2} \left(\frac{1 + \cos^2\theta}{2} + 2g \cos\theta \right), \quad (16) \end{aligned}$$

where $\mathbf{S}^{\text{scat}} = (1/2)\text{Re}\{\mathbf{E}^{\text{scat}*} \times \mathbf{H}^{\text{scat}}\}$ is the time averaged Poynting vector, $|\alpha_{\text{sum}}|^2 \equiv |\alpha_E|^2 + |\alpha_M|^2$ and

$$g = \frac{\text{Re}\{\alpha_E \alpha_M^*\}}{|\alpha_{\text{sum}}|^2} \quad (17)$$

is the so-called asymmetry factor [19] for dipolar electric and magnetic scatterers [16, 30].

Although in the strict far field limit the flow lines of \mathbf{S}^{scat} lie along the spherical radial direction, tracing them to their source, they do indeed spiral towards the origin in analogy with the light scattered by an electric dipole excited by circularly polarized light [14, 31–34]. Consequently, as sketched in Fig. 1, the full Poynting vector \mathbf{S}^{scat} makes an angle with the line of sight, which determines an apparent shift Δ in the perceived position of the particle, with

$$\Delta = \lim_{kr \rightarrow \infty} -r \left(\frac{\mathbf{S}^{\text{scat}} - \hat{\mathbf{e}}_r (\hat{\mathbf{e}}_r \cdot \mathbf{S}^{\text{scat}})}{|\mathbf{S}_r|} \right) \quad (18)$$

$$= \lim_{kr \rightarrow \infty} \left(\frac{\hat{\mathbf{e}}_r \times (\mathbf{r} \times \mathbf{S}^{\text{scat}})}{|\mathbf{S}_r|} \right) \quad (19)$$

$$= \lim_{kr \rightarrow \infty} \left(\frac{2i}{k} \frac{\mathbf{E}_\sigma^{\text{scat}*}}{|\mathbf{E}_\sigma^{\text{scat}}|^2} \frac{\partial \mathbf{E}_\sigma^{\text{scat}}}{\partial \varphi} \right) \hat{\mathbf{e}}_\varphi \quad (20)$$

where $\mathbf{E}_\sigma^{\text{scat}}$ is given by Eqs. (12) and (13). Taking into account Eq. (11), the apparent shift can be written as

$$\frac{\Delta}{(\lambda/\pi)} = -\frac{\ell_z(\theta)}{\sin\theta} \hat{\mathbf{e}}_\varphi = \frac{s_z(\theta) - \sigma}{\sin\theta} \hat{\mathbf{e}}_\varphi \quad (21)$$

$$= -\sigma \left[\frac{\sin\theta (1 + 2g \cos\theta)}{1 + \cos^2\theta + 4g \cos\theta} \right] \hat{\mathbf{e}}_\varphi. \quad (22)$$

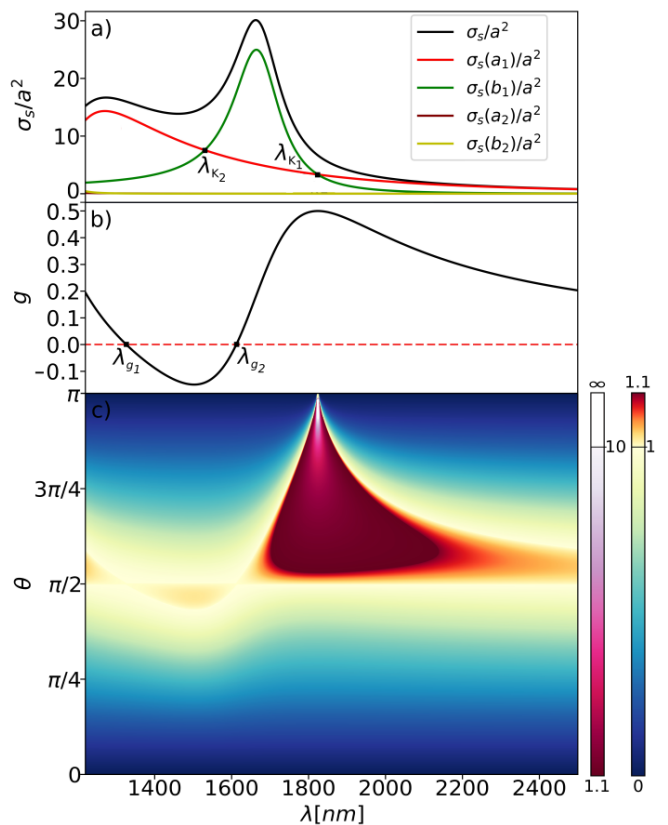


FIG. 3: (a) Scattering cross sections σ_s for a 230 nm Si nanosphere versus the wavelength. The special wavelengths $\lambda_{K_1} = 1825$ nm and $\lambda_{K_2} = 1520$ nm correspond to first and second Kerker conditions, respectively. (b) Asymmetry factor versus the wavelength. This is identical to zero at $\lambda_{g_1} = 1326$ nm and $\lambda_{g_2} = 1612$ nm (and negative in between). The maximum value is localized at the first Kerker condition, namely, λ_{K_1} . (c) Colormap of the normalized optical mirage, $\Delta/(\lambda/\pi)$, versus the scattering angle and the wavelength. The maximum enhancement for λ_{K_1} at backscattering ($\theta = \pi$) is clearly observed.

This is the first important result of this Letter: the shift is always along $\hat{\mathbf{e}}_\varphi$, perpendicular to the incidence plane and proportional to the z -component of the OAM per photon. Importantly, the sign of the displacement is purely determined by the incoming helicity.

In absence of magnetic dipolar response, setting $g=0$ in Eq. (22), one recovers the previously reported results for electric dipoles [14, 34], which were interpreted as a result of transfer from SAM to OAM [14, 35]. According to those previous works, this transfer is expected to be maximum at those directions at which the scattered light is linearly polarized (being the SAM of scattered photons identically zero). For an electric dipole excited by circularly polarized light the maximum transfer would take place in the plane perpendicular to the incoming light ($\theta = \pi/2$) being the maximum displacement equal to

$$\Delta = \lambda/\pi.$$

The fields scattered by electric and magnetic dipoles present a very different polarization structure [36, 37]. Contrary to the purely electric (or magnetic) case, when excited with a circularly polarized field, the scattered radiation on the plane perpendicular to the incoming light ($\theta = \pi/2$) is no longer linearly polarized. Interestingly, this change does not affect the streamlines of the Poynting vector on this particular plane (as shown in Fig. 2), leading to the same subwavelength optical mirage. However, out of this plane the apparent displacement presents a peculiar behaviour that strongly depends on both θ and the wavelength.

Figures 3 and 4 summarize the anomalous behavior of the apparent displacement $\Delta(\lambda, \theta)$ for silicon nanospheres in the infrared (similar behavior is obtained in other spectral ranges as long as the scattering cross section can be described by only the first two dipolar multipoles, see Fig. 3a). As it can be seen in Figure 4, for $\theta = \pi/2$ the displacement is always λ/π for all wavelengths. When the asymmetry factor g is negative ($\lambda_{g1} < \lambda < \lambda_{g2}$) the maximum displacement occurs for $\theta < \pi/2$ and it is always subwavelength but slightly larger than the one for $\theta = \pi/2$. However, for $g > 0$ the apparent displacement can be much larger than λ/π and when the electric and magnetic polarizabilities are identical ($\lambda = \lambda_{K1}$), i.e. at the so-called first Kerker condition, it diverges as $\theta \rightarrow \pi$. Notice that the singularity is resolved naturally since at the first Kerker condition there is exactly zero back-scattered intensity.

We can now examine the peculiar behaviour of Δ near the first Kerker condition in terms of the angular momentum flow. When the electric and magnetic responses are identical, i.e. $\alpha_E = \alpha_M$, the system is “dual” and the scattering preserves helicity [38, 39]. In this case, the asymmetry factor is maximum, $g = 1/2$, (see Fig 3b) which leads to $s_z(\theta) = \sigma \cos \theta$ and

$$\frac{\Delta\pi}{\lambda_{K1}} = -\sigma \tan\left(\frac{\theta}{2}\right) \hat{e}_\varphi. \quad (23)$$

From this equation two interesting limiting cases can be identified: firstly, in the forward direction the optical mirage and l_z go to zero since $\mathbf{S}_\varphi = 0$. This can alternatively be understood by means of the symmetries of the system: being the scatterer dual, the system must conserve the helicity of the incoming field, which in the forward direction corresponds to the spin density. Thus, the incident circular polarization is preserved in the forward direction and must carry all the angular momentum density (leaving $l_z=0$). Secondly, in the direction perpendicular to the incident wave-vector ($\theta = \pi/2$), the interference term vanishes. As a consequence, $s_z = 0$ and $l_z = \sigma$ and, in analogy with electric dipoles, we obtain $\Delta = \sigma\lambda/\pi$, although in that case light in this direction is fully circularly polarized (see Fig. 2).

The most striking effect arises at an observation angle near backscattering $\theta \lesssim \pi$ where, as discussed above,

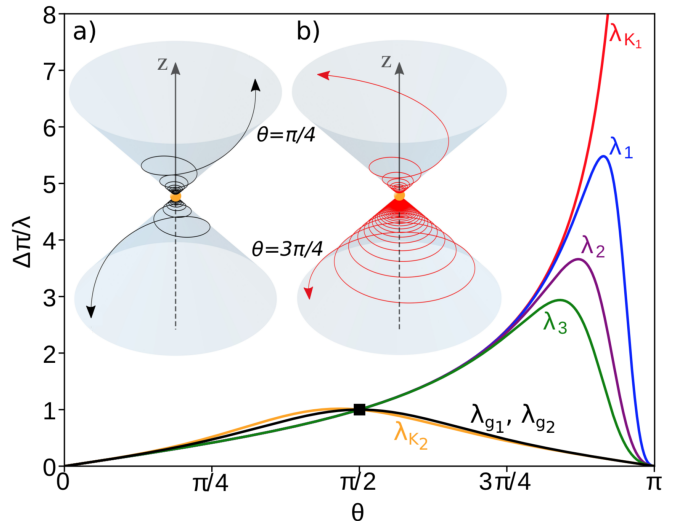


FIG. 4: Optical mirage colormap (Fig. 3) cuts versus the scattering angle for different values of the wavelength, belonging to regions with $g < 0$ (λ_{K2}), $g = 0$ ($\lambda_{g1}, \lambda_{g2}$) and $g > 0$ (λ_1, λ_2 and λ_3 , respectively decreased 5, 10 and 15 nm with respect to λ_{K1} , and λ_{K1} itself). At $\theta = \pi/2$, $\Delta = \lambda/\pi$ is observed to be a universal value. Both subplots show examples of trajectories of the Poynting vector at forward and backscattering, being similar for λ_{g1} and λ_{g2} (a) and considerably different for λ_{K1} (b).

the apparent displacement diverges. This divergence is solved because the Poynting vector becomes strictly zero at backscattering, which suggests the appearance of an optical vortex in that direction. As a matter of fact, near backscattering $l_z(\lesssim \theta) \rightarrow 2\sigma$, while the spin reverses sign $s_z(\theta \lesssim \pi) \rightarrow -\sigma$ (but still maintaining constant helicity), which confirms the existence of a vortex with $l = 2\sigma$ emerging from a nanoparticle as a nanoscale analogue of the light backscattered from a perfect reflecting cone [40].

In conclusion, we have shown that light scattering from dipolar electric and magnetic nanoparticles, excited by circular polarized light, can lead to optical mirages values much larger than the incident wavelength. The properties of the optical mirage were discussed in terms of spin-orbit interactions and helicity conservation. Interestingly, for dual spheres, i.e. at the so-called first Kerker condition, we predicted a huge enhancement of the apparent shift related to the emergence of an optical vortex in the backscattering direction.

This research was supported by the Spanish Ministerio de Economía y Competitividad (MICINN) and European Regional Development Fund (ERDF) Projects FIS2014-55987-P, FIS2015-69295-C3-3-P and FIS2017-82804-P, by the Basque Dep. de Educación Project PI-2016-1-0041 and by Basque Government ELKARTEK program through MICRO4FAB (KK-2016/00030) and $\mu 4F$ (KK-2017/00089) Projects. A. G.-E. received funding from the Fellows Gipuzkoa fellowship of the Gipuzkoako Foru

Aldundia through FEDER "Una Manera de hacer Europa" .

Jorge Olmos-Trigo and Cristina Sanz-Fernández contributed equally to this work.

-
- [1] L. Allen, S. M. Barnett, and M. J. Padgett, *Optical angular momentum* (CRC Press, 2003).
- [2] V. Liberman and B. Zel'dovich, *Phys. Rev. A* **46**, 5199 (1992).
- [3] J. H. Crichton and P. L. Marston, *Electron. J. Differ. Eq.* **4**, 37 (2000).
- [4] M. Berry, M. Jeffrey, and M. Mansuripur, *J. Opt. A: Pure Appl. Opt.* **7**, 685 (2005).
- [5] K. Y. Bliokh, F. Rodríguez-Fortuño, F. Nori, and A. V. Zayats, *Nat. Photonics* **9**, 796 (2015).
- [6] M. Dyakonov and V. Perel, *Phys. Lett. A* **35**, 459 (1971).
- [7] J. Hirsch, *Phys. Rev. Lett.* **83**, 1834 (1999).
- [8] L. Berger, *Phys. Rev. B* **2**, 4559 (1970).
- [9] M. I. Dyakonov and A. Khaetskii, in *Spin physics in semiconductors* (Springer, 2008) pp. 211–243.
- [10] J. Sinova, S. O. Valenzuela, J. Wunderlich, C. Back, and T. Jungwirth, *Rev. Mod. Phys.* **87**, 1213 (2015).
- [11] M. Onoda, S. Murakami, and N. Nagaosa, *Phys. Rev. Lett.* **93**, 083901 (2004).
- [12] K. Y. Bliokh and Y. P. Bliokh, *Phys. Rev. Lett.* **96**, 073903 (2006).
- [13] O. Hosten and P. Kwiat, *Science* **319**, 787 (2008).
- [14] D. Haefner, S. Sukhov, and A. Dogariu, *Phys. Rev. Lett.* **102**, 123903 (2009).
- [15] M. Kerker, D.-S. Wang, and C. Giles, *J. Opt. Soc. Am. A* **73**, 765 (1983).
- [16] M. Nieto-Vesperinas, R. Gomez-Medina, and J. J. Saenz, *J. Opt. Soc. Am. A* **28**, 54 (2011).
- [17] R. Gómez-Medina, B. Garcia-Camara, I. Suárez-Lacalle, F. González, F. Moreno, M. Nieto-Vesperinas, and J. J. Sáenz, *J. Nanophotonics* **5**, 053512 (2011).
- [18] J. D. Jackson, *Classical Electrodynamics* (John Wiley & Sons, New York, 1999).
- [19] C. F. Bohren and D. R. Huffman, *Absorption and scattering of light by small particles* (John Wiley & Sons, 2008).
- [20] I. Fernandez-Corbaton, X. Zambrana-Puyalto, and G. Molina-Terriza, *Phys. Rev. A* **86**, 042103 (2012).
- [21] X. Zambrana-Puyalto, I. Fernandez-Corbaton, M. Juan, X. Vidal, and G. Molina-Terriza, *Opt. Lett.* **38**, 1857 (2013).
- [22] N. Tischler, X. Zambrana-Puyalto, and G. Molina-Terriza, *Eur. J. Phys.* **33**, 1099 (2012).
- [23] A. B. Evlyukhin, C. Reinhardt, A. Seidel, B. S. Luk'yanchuk, and B. N. Chichkov, *Phys. Rev. B* **82**, 045404 (2010).
- [24] A. García-Etxarri, R. Gómez-Medina, L. S. Froufe-Pérez, C. López, L. Chantada, F. Scheffold, J. Aizpurua, M. Nieto-Vesperinas, and J. J. Sáenz, *Opt. Express* **19**, 4815 (2011).
- [25] J.-M. Geffrin, B. García-Cámara, R. Gómez-Medina, P. Albella, L. S. Froufe-Pérez, C. Eyraud, A. Litman, R. Vaillon, F. González, M. Nieto-Vesperinas, J. J. Sáenz, and F. Moreno, *Nat. Commun.* **3**, 1171 (2012).
- [26] S. Person, M. Jain, Z. Lapin, J. J. Sáenz, G. Wicks, and L. Novotny, *Nano Lett.* **13**, 1806 (2013).
- [27] Y. H. Fu, A. I. Kuznetsov, A. E. Miroshnichenko, Y. F. Yu, and B. Luk'yanchuk, *Nat. Commun.* **4**, 1527 (2013).
- [28] L. Shi, J. T. Harris, R. Fenollosa, I. Rodriguez, X. Lu, B. A. Korgel, and F. Meseguer, *Nat. Commun.* **4**, 1904 (2013).
- [29] A. I. Kuznetsov, A. E. Miroshnichenko, M. L. Brongersma, Y. S. Kivshar, and B. Luk'yanchuk, *Science* **354**, aag2472 (2016).
- [30] R. Gómez-Medina, L. Froufe-Pérez, M. Yépez, F. Scheffold, M. Nieto-Vesperinas, and J. J. Sáenz, *Phys. Rev. A* **85**, 035802 (2012).
- [31] W. Gough, *Eur. J. Phys.* **7**, 81 (1986).
- [32] H. F. Arnoldus and J. T. Foley, *Opt. Commun.* **231**, 115 (2004).
- [33] C. Schwartz and A. Dogariu, *Opt. Lett.* **31**, 1121 (2006).
- [34] H. F. Arnoldus, X. Li, and J. Shu, *Opt. Lett.* **33**, 1446 (2008).
- [35] K. Y. Bliokh, E. A. Ostrovskaya, M. A. Alonso, O. G. Rodríguez-Herrera, D. Lara, and C. Dainty, *Opt. Express* **19**, 26132 (2011).
- [36] A. García-Etxarri, *ACS Photonics* **4**, 1159 (2017).
- [37] A. García-Etxarri and J. A. Dionne, *Phys. Rev. B* **87**, 235409 (2013).
- [38] I. Fernandez-Corbaton, X. Zambrana-Puyalto, N. Tischler, X. Vidal, M. L. Juan, and G. Molina-Terriza, *Phys. Rev. Lett.* **111**, 060401 (2013).
- [39] M. K. Schmidt, J. Aizpurua, X. Zambrana-Puyalto, X. Vidal, G. Molina-Terriza, and J. J. Sáenz, *Phys. Rev. Lett.* **114**, 113902 (2015).
- [40] M. Mansuripur, A. R. Zakharian, and E. M. Wright, *Phys. Rev. A* **84**, 033813 (2011).